CASL-U-2013-0099-000

Power uprates
and plant life extension

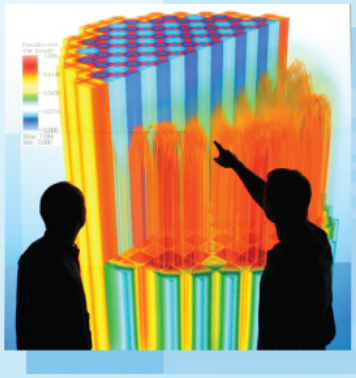

Engineering design
and analysis

Science-enabling
high performance
computing

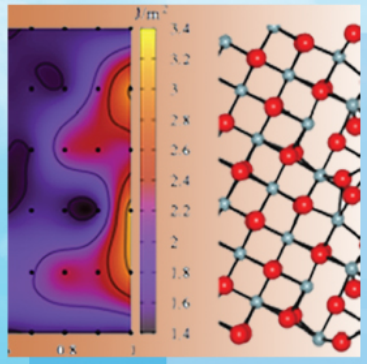

Fundamental science

Plant operational data

Consortium for Advanced Simulation of LWRs

Advancements on Wall Boiling Modeling in CFD: Leveraging New Understanding from MIT Flow Boiling Facility

Massachusetts Institute of Technology

L Gilman and E. Baglietto

May 12-17, 2013:

U.S. DEPARTMENT OF ENERGY | Nuclear Energy

ADVANCEMENTS ON WALL BOILING MODELING IN CFD: LEVERAGING NEW UNDERSTANDING FROM MIT FLOW BOILING FACILITY

L. Gilman[1] and E. Baglietto[1]
[1]Massachusetts Institute of Technology Department of Nuclear Science and Engineering,
138 Albany Street, NW12-236, Cambridge, MA 02139, USA

lgilman@mit.edu,emiliob@mit.edu

ABSTRACT

The fundamental target of this work is to introduce all necessary mechanisms to accurately predict the temperature and heat flux for subcooled flow boiling at the wall in CFD simulations.Comparisons between numerical predictions and experimental data have illustrated an excessively high sensitivity of critical closure parameters on local conditions, which are not replicated in the experiments. This evidence suggests the need for an improved, more general boiling heat transfer model that will show more consistent dependency on local parameters and include an improved description of flow effects on surface boiling. Some innovative ideas are introduced and the evaluation and experiment-based development approach is presented in this paper that focuses on the wall boiling phenomena. A new description for the evaporation heat flux is introduced, together with a more realistic representation of the active nucleation site and description of dry surface area during boiling. The effects of bubble slidingare introduced to extend model applicability and the quenching component in the heat partitioning model is modified to include its dependence on the wall material.

Further, some preliminary studies are shown to demonstrate the influence of the boiling on both wall friction and heat transfer as a further component of model improvement. A simple analysis adopting the quasi-DNS data from the CASL ITM-1 results illustrates the change in heat transfer coefficient in single-phase fluid flow whenthe surface roughness is modified to capture the presence of bubbles for a high-Reynolds number condition.

1. INTRODUCTION AND MOTIVATION

In many industrial applications, subcooled flow boiling is used when a high heat transfer coefficient is desired. In order to maintain this efficient heat transfer regime,the critical heat flux, which is dependent on the geometry and flow conditions, must be avoided. The need to verify optimal flow conditions for new and enhanced designs has driven studies in numerical analyses, such as CFD, to replace the use of experiments.

To correctly describe critical heat flux using CFD, a complete understanding of the complex boiling phenomena and boiling mechanisms needs to be assembled. A flow boiling facility is available at MIT, where non-invasive techniques are used to capture new and unique subcooled flow boiling data on multiple parameters simultaneously. This facility was specifically constructed to support advanced CFD model development and it provides a complete new look at the boiling phenomenon. The experimental measurements have provided clarification of

shortcomings of current model approaches, and most importantly, are providing fundamental data to suggest new thinking that will provide a more general and robust representation.

Comparisons between CFD predictions and experimental data [1],[2],[3] have illustrated the high sensitivity of current boiling closure parameters such as bubble departure diameter, bubble departure frequency, and active nucleation site density on factors such as the wall superheat. Tolubinsky and Kostanchuk[4] predicted thebubble departure diameter byrelating it to the degree of local liquid subcooling, which has been used with some success for a limited set of flow parameters. Another model by Kocamustafaogullari[5] suggests that a force balance between gravity and surface tension forces can be used to predict the departure diameter, but this model has been used with limited success in CFD simulations.

The bubble departure frequency model by Cole [6] predicts the frequency by relating it to the typical bubble rise velocity and the bubble departure diameter. More recently proposed bubble departure frequency calculations use the ebullition cycle and account for both the waiting time prior to bubble inception and the time period of bubble growth [7].

The simulation of vapor generation for wall boiling using CFD is extremely sensitive to the active nucleation site density closure parameter. To predict the wide ranges in experimental data for active nucleation site density for a given wall superheat, a dependence on the static contact was added [8] to the model and has been incorporated into the Hibiki and Ishii model [9]. Even with the contact angle dependency, the active nucleation site density models have difficulty capturing the number of active nucleation sites seen experimentally.To remove this dependency on active nucleation site density correlations,a fractal method was developed that treats the active cavity sites analogous to pores in a porous media [10].

There are various approaches for modelling two-phase flow using CFD. The Eulerian MultiPhase (EMP) framework represents the most promising method to model boiling in complex industrial applications. The wall boiling representation in this framework is nevertheless still relying on the classic heat partitioning concept introduced by Judd and Hwang (1976)[11]and adapted by Kurul and Podowski (1990) [12]. This is shown in(1) where the total heat flux (q''_{tot}) is partitioned into convection (q''_{fc}), quenching, which captures the heat expended in the re-formation of the disrupted thermal boundary from bubble departure (q''_q), and the latent heat of evaporation (q''_e) components. While the model has shown great flexibility thanks to its detailed mechanistic approach, its ability to correctly predict some of the model parameters in realistic conditions is still challenged.Additionally, some of the fundamental physical characteristics of boiling are not captured in this partitioning and this can strongly limit the applicability and generality of the approach.

$$q''_{tot} = q''_{fc} + q''_q + q''_e \tag{1}$$

The movement of bubbles on the heater surface prior to lift-off is not captured in this heat partitioning approach by Kurul and Podowski (1990) since it does not consider the effects of sliding bubbles along the wall[13] which has been shown to occur in subcooled flow boiling through experiments [14],[15]. In subcooled boiling, bubbles often slide along the heated wall after detaching from the nucleation site and before lifting off into the bulk of the liquid flow.

These sliding bubbles can also merge and coalesce with other detached and nucleating bubbles downstream. The tendency for bubble sliding is high in subcooled flow boiling and as a result, efforts have been made to incorporate the transient conduction of sliding bubbles in the heat partitioning model[7],[13].

To incorporate the effects of sliding bubbles in heat transfer, a fundamental theory is being investigated. An interesting opportunity is the possibility of using a mechanistic force balance model to predict when a bubble will begin to slide along the heated wall, in the same fashion as it is currently used to predict bubble departure diameter. The original concept was proposed for both pool and flow boiling by Klausner et al. [16] and Zeng et al. [17] and it was recentlyadapted and modified by Yun et al.[18]for CFD application. Although advancements have been made in parameter calculations in subcooled flow boiling modelling using CFD, the need is still present for a modified, more general heat transfer model that uses less sensitive closure parameters and considers flow effects on boiling.

2. BASELINE BOILING MODEL

The testing and implementation of the proposed general boiling model is completed using the commercially available STAR-CCM+ software. The EMP framework using the two-fluid, six-equation method is employed in the software tomodel two-phase flow and is discussed below.

The wall boiling model used is the classic heat partitioning model by Kurul and Podowski as shown in (1). In the simulation, the total heat flux is computed as the sum of the partitioned components. The convection term describes the removal of heat by single-phase turbulent convection and is shown in (2). The quenching term describes the enhancement of heat transfer due to the replacement of a departing bubble by an influx of cooler liquid and is shown in (3). The Del Valle and Kenning model is used to determine quenching heat transfer coefficient and is shown in (5).The wait time (t_w) is determined using a wait coefficient that comes from the Kurul and Podowski assumption that quenching occurs between the departure of one bubble and the nucleation of the next. The influence wall area fraction (K_{quench}) also follows the Kuruland Podowski standard model. The evaporation heat flux is shown in (4). The bubble departure diameter, active nucleation site density, and frequency for bubble departure are determined by correlations. When using the Hibiki and Ishii model, a limit is applied to the amount of superheat that can be applied to prevent unrealistic values for N'', which is an important parameter that will be further discussed in the model development. The imposed maximum wall superheat default value is typically ~25K.

$$q''_{fc} = h_{fc}(\Delta T_w + \Delta T_{sub}) \tag{2}$$

$$q''_q = h_{quench}(\Delta T_w + \Delta T_{sub}) \tag{3}$$

$$q''_e = \rho_v h_{fg} \frac{\pi}{6} D_d^3 N'' f \tag{4}$$

$$h_{quench} = 2K_{quench} f \sqrt{\frac{\rho_l c_{pl} k_l t_w}{\pi}} \tag{5}$$

The bulk boiling/condensation is driven by the heat transfer between phases. The heat transfer coefficient for the gas side uses a constant value and the liquid side adopts the Ranz-Marshall correlation [19]. A population balance model can also be implemented to better predict bubble size and distribution in a heated channel.

3. PROPOSED HEAT TRANSFER MODELING BY BOILING REGIME

The following subsections describe the physical phenomena and the proposed method to model them in each boiling regime encountered in subcooled flow boiling.

3.1 Prior to Bubble Formation

The first regime in subcooled flow boiling is the region prior to bubble formation on the heated wall and is illustrated in Figure 1. Therefore, the total heat flux in the proposed method is captured in the single-phase forced convection component as shown in (6).

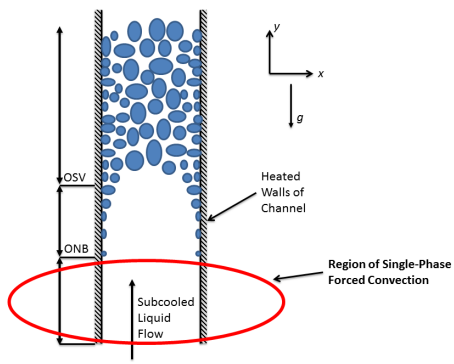

Figure 1 – Illustration of a heated channel for the single-phase region in subcooled flow boiling.

$$q''_{tot} = q''_{fc} = h_{fc}(\Delta T_w + \Delta T_{sub}) \tag{6}$$

3.2 Between Onset of Nucleate Boiling (ONB) and Onset of Significant Voids (OSV)

3.2.1 Presence of Static Bubbles

In this regime, bubbles form and remain attached to the heated surface due to the flow conditions that form the thermal boundary. This prevents bubbles from reaching the bubble departure diameter and therefore they remain attached to the heater.Experiments have shown that the initial bubble growth is rapid and condensation occurs at the top of the bubble [20],[21].

This regime partitions the heat flux into two components given by (7). The first component is the single-phase forced convection term (q''_{fc}) employed on the heated area not under the area of influence of the bubbles. The addition of the bubbles changes the surface roughness in this regime resulting in enhanced forced convection heat transfer because of the roughness and the oscillations at the liquid-vapor interface. This enhanced convective heat transfer is also described

and captured in a method by Basu et al.[7]and this modified forced convection term is shown in (8).

$$q''_{tot} = q''_{fc} + q''_{e} \tag{7}$$

$$q''_{fc} = h_{fc} H_{corr} (\Delta T_w + \Delta T_{sub}) \tag{8}$$

Here, H_{corr}captures the enhanced heat transfer due to the presence of bubbles on the heater surface. It is a function of the number and size of bubbles on the heater surface. To quantify the effect of the increased heat transfer due to the increased roughness, a study was completed where the bubbles were treated as hemispherical obstacles on the heater surface. This allowed for their effect to be included in a simulation by using an influence of wall roughness by modification to the adopted wall function and a preliminary study is discussed in Section 4.

The evaporation component (q''_e) captures the fraction of energy from the superheated liquid layer that is used for evaporation. To capture this heat transfer phenomenon, the evaporation term employs a microlayer evaporation model, such as the model currently under development at MIT. This term is dependent on the microlayer thickness, the time required to evaporate the microlayer, and the fraction of area taken up by the microlayer on the heated surface. The current partitioning approach, which estimates the evaporation term from bubble departures does, in fact, not include this microlayer contribution.

The microlayer is a thin layer of liquid that becomes trapped between a quickly growing bubble and the superheated wall and is illustrated in Figure 2. The evaporation of the microlayer of liquid between the bubble and the wall has been studied through experiments using interferometry and high-speed cinematography [22], [23], [24]. These have illustrated that microlayer evaporation plays a significant role even in low subcooling conditions.

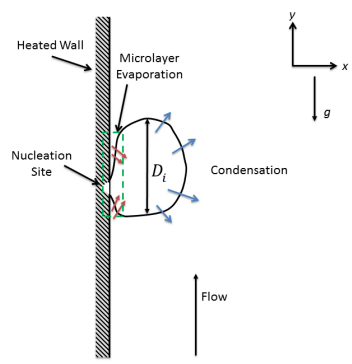

Figure 2 – Illustration of microlayer evaporation and condensation on a bubble attached to a heated wall.

As mentioned above, the total area under the influence of forced convection is determined by subtracting the area influenced by evaporation: $A_{fc} = A_h - A_{ev}$, where$A_h$is the total heated area in this region. Current models calculate the area under the influence of evaporation (A_{ev}) by using the bubble size (A_b), active nucleation site density (N''), and an influence area term (F_A).

The area of influence term takes into account that the bubble on the heater surface affects an area larger than the physical area of the bubble. It must also account for "crowding" when the number of bubbles on the heater surface begin to affect each other [25]. Using this formulation, $A_{ev} = F_A N'' A_b$. Instead, in this proposed model, the evaporation area is related to a more general parameter that is calculated dependent on the boiling regime- the dry surface area (S_{dry}) such that$S_{dry} = N'' A_{dry,spot} K_{corr}$.

The factor K_{corr} is used to enforce a correct limiting behavior of the available dry surface area rather than imposing a maximum wall superheat, which is currently done in CFD simulations to prevent an unphysical high active nucleation site density. Then the calculation for the evaporation area becomes $A_{ev} = F'_A S_{dry}$.

Literature sources vary on the reported size of the influence area factor [11],[12] which consequently affects the number of bubbles that can fit on the heater surface. Once this maximum number of active nucleation sites is reached, and is depicted inFigure 3, the determination of the dry surface area must change by altering K_{corr}.This figure also illustrates the dry surface area ($A_{dry,spot}$), microlayer area (S_{ML}), and the influence area (F'_A) of a single bubble. Additional experimental data will be studied to determine the parameters that affect F'_A. An illustrative graph to show how the K_{corr} will be used to suppress the drastic increase in active nucleation site density at high wall superheat and better depict the amount of dry surface area is depicted in Figure 4.

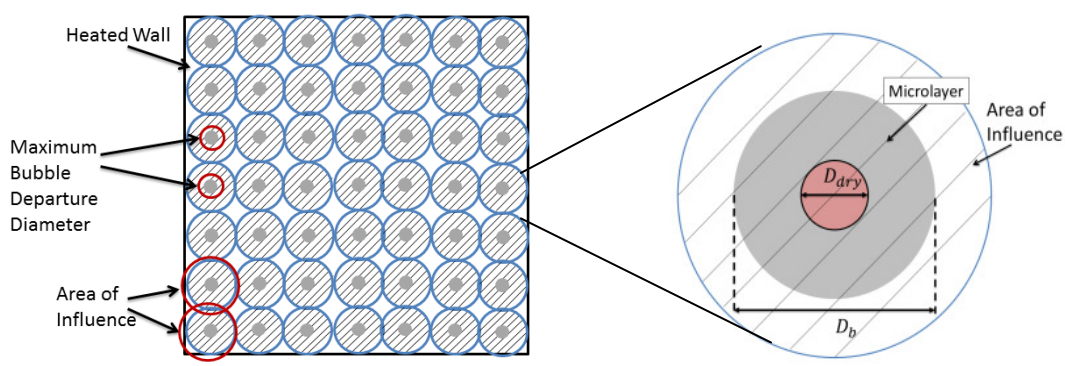

Figure 3 – Illustration of the maximum number of active nucleation sites on a heated surface with a magnified view to show the dry area, microlayer area, and the area of influence for a single bubble.

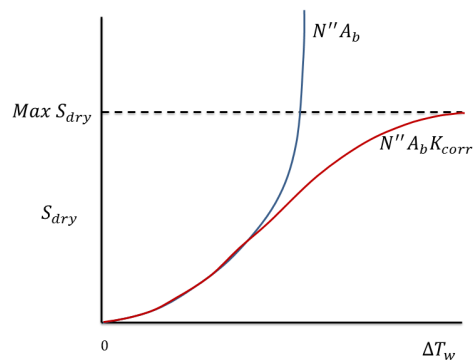

Figure 4 – Illustration of the increase in dry surface area to the maximum value, which is equal to the area of the heater.

3.2.2 Bubble Departure and Sliding without Bubble Merging

Bubble movement and departure from the nucleation site occurs in this regime. The bubble departure diameter (D_d) is defined as the diameter of the bubble when it moves from its inception point, or point of origin. At this size, the bubble slides along the heater surface and lifts off when it reaches the lift-off diameter size (D_l). A bubble may reach D_l immediately after D_d so that it lifts off into the fluid flow without sliding.

Four components make up the heat flux partitioning model in this regime by the addition of the transient conduction (q''_{tc}) and quenching (q''_{quench}) components as is shown in(9). The q''_{fc} is calculated as described in section 3.2.1 but is only active when not influenced by a sliding bubble. The q''_e is calculated using the microlayer evaporation model.

$$q''_{tot} = q''_{fc} + q''_e + q''_{tc} + q''_{quench} \tag{9}$$

Transient conduction occurs because of the disruption of the thermal boundary layer. This disruption occurs both through bubble lift-off and sliding. It is assumed that when the boundary layer is disrupted q''_{tc} occurs for some time interval while the thermal boundary layer is re-established and is implemented in the areas swept by bubbles. The component is calculated similar to the enhanced forced convection using a different enhancement factor dependent on the number of bubbles and the time over which the transient conduction mode occurs and is shown in (10).

$$q''_{tc} = h_{fc}B_{corr}(\Delta T_w + \Delta T_{sub}) \tag{10}$$

The quenching term is governed by the heated material because this heat transfer mode involves bringing the influence area of the bubble on the heater back to the wall superheat and temperature distribution prior to the next bubble inception. In this method, the quenching term becomes a function of the material properties of the heated surface. It is employed when a bubble departs from its nucleation site and depicted in Figure 5.The quenching heat flux is shown in (11)where ρ_h is the density of the heater material, $c_{p,h}$ is the heat capacity, T_a is the average temperature in the hot spot on the heater in the bubble location, and δ_h is the average depth of the hot spot. The temperature and depth of the area will be determined using the thermal

conductivity of the material and the temperature of the microlayer. For the heat flux over the heater, the quenching component is dependent on the dry surface area.

$$q''_{quench} = \rho_h c_{p,h}(T_a - T_w)\delta_h \tag{11}$$

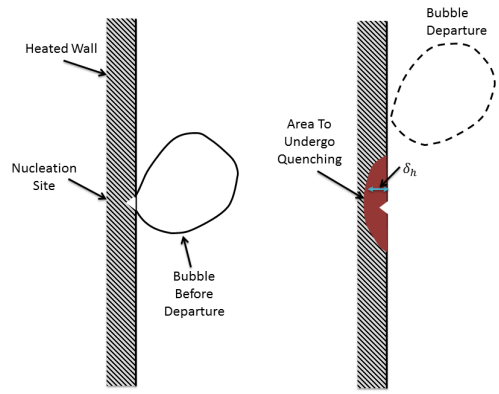

Figure 5 – Illustration of bubble growth on a heater and the area in the influence of the bubble that is involved in the quenching heat flux.

To quantify the area affected by sliding bubbles, for simplicity, an even distribution of bubbles on the heater in a square grid is assumed so that the distance between bubbles, s, is given by $s = 1/\sqrt{N''}$. It is also assumed that bubbles slide only in the direction of the flow. Bubble growth can still occur while the bubble is sliding and is depicted in Figure 6for data collected at the MIT flow boiling facility. The sliding distance is defined as l_0 which is the distance a bubble will travel as it grows from $D_d$to D_l. Thus when a bubble slides without merging, $s > l_0$ and defining the actual sliding distance as l, $l = l_0$ in this case and is depicted in Figure 7. The sliding distance is important for the calculation of the transient conduction.

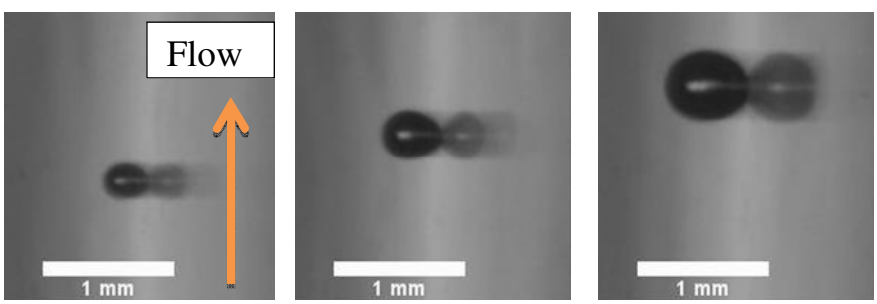

Figure 6 – Illustration of a bubble sliding captured at the MIT Flow Boiling Facility by Bren Phillips. Test was completed using water at atmospheric pressure, heat flux of 130 kW/m^2, and 10°C subcooling.

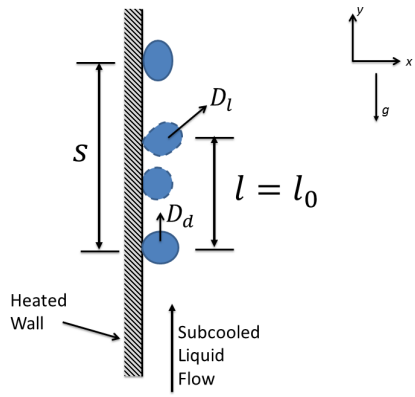

Figure 7 – Illustration of a bubble sliding from its inception point and then departing from the heater.

3.2.3 Bubble Sliding with Bubble Coalescence on the Heater

In this region, enough bubbles are present on the heater that the sliding bubbles coalesce on the heater surface as depicted in Figure 8. The heat flux portioning is comprised of the four components shown in (9).

Since bubbles merge on the heater surface prior to lift-off,$s \leq l_0$. The primary sliding bubble gains the vapor volume of the secondary bubble it merges with and bubbles that coalesce on the heater surface lift-off together[20], [21]. Additionally, the bubble merging causes the actual number of bubbles departing from the heater surface to be less than N'' and this is accounted for by using a reduction factor (R_f) given by (12). This is the number of bubbles lifting off per unit area of the heater over the number of active nucleation sites per unit area. The number of bubbles departing affects the transient conduction calculation since it captures the reformation of the thermal layer near the wall.It also changes the calculation of S_{dry} since the K_{corr} term is active in this region to accurately predict the dry surface area.

$$R_f = 1/(l\sqrt{N''}) \tag{12}$$

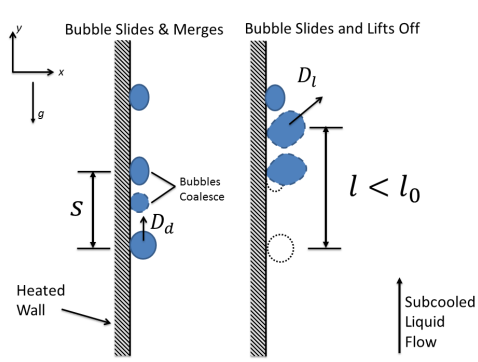

Figure 8 – Illustration of bubbles sliding and merging on the heater surface before lifting off into the fluid.

3.3 Onset of Significant Voids

In this regime, the high void generation causes many bubble interactions on the heater surface. The heat partitioning given by (9) and the importance of the forced convection component will decrease significantly while transient conduction increases. The main heat transfer mode in this region involves the evaporation term and therefore, the evaporation surface and dry surface quantification are the most important parameters and need to be verified through further testing. Completed experiments have illustrated that even at high void generation, no single fraction of the heated surface remains dry due to liquid sloshing [23]. The dependence on the dry surface area in this proposed model allows for a natural way to extend the model to predict departure from nucleate boiling (DNB).

4. BUBBLE INFLUENCE ON HEAT TRANSFER COEFFICIENT

In the ITM-1 study [26], the effect of bubbles attached to a wall on both the near-wall turbulence and the friction factor were investigated using the code TransAT. Both Direct Numerical Simulation (DNS) and Large Eddy Simulation (LES) approaches were used to resolve the flow. The bubbles were modeled as hemispherical solid obstacles of height k (equivalent to y+ = 10) on the walls of the simulation domain. They are spaced at a distance S_b equivalent to y+ = 40 and arranged on a square lattice. The simulation was completed using an imposed shear Reynolds number (Re_τ) of 400, a fixed density (ρ) of 1 kg/m^3, and viscosity (μ) of Re_τ^{-1}.

In the hydraulically smooth wall case, the expressions adopted are the traditional wall functions for a high-Reynolds-number and shown in(13). The empirical coefficient (E) is usually set equal to 9.0 and is a constant from the rearrangement of the classic equation (14)to give$E = e^{KB}$, where K is the Von Karman constant.

$$u^+ = y^+ \qquad when\, y^+ \leq y_m^+ \tag{13}$$

$$u^+ = \frac{1}{K}\ln\left(Ey^+\right) \quad when\, y^+ > y_m^+$$

$$u^+ = \frac{1}{K}\ln(y^+) + B \tag{14}$$

Using the smooth wall correlation, the empirical coefficient was modified to obtain the wall function shape that was determined in ITM Test Case 1 for hemispherical obstacles. The dimensionless velocity for both the ITM Test Case and the modified smooth wall function were found to be in good agreement when $E = 3.4$.

The effect of this wall function modification on the heat transfer coefficient was investigated by comparing the single-phase heat transfer coefficient on smooth and rough walls in STAR-CCM+ on a 1 m long test section with a rectangular flow area of 30 mm x 10 mm (300 mm^2) at atmospheric pressure. A constant heat flux of 200 kW/m^2 was implemented on a 10 mm x 20 mm heater section of the channel, the inlet velocity was 1.2 m/s with 10°C liquid subcooling. This allowed for a maximum wall superheat of 18-19°C to be reached and when a two-phase model

was implemented the maximum void fraction on the heater was 0.009 on only a small fraction of the heater (<4%). A comparison of the heat transfer coefficient of the smooth and rough walls is shown in Figure 9. This illustrates the change in single-phase forced convection due to the presence of bubbles on the heater wall where the increased roughness increases the heat transfer coefficient. The wall function was modified only on the heater area where the bubbles would be present.

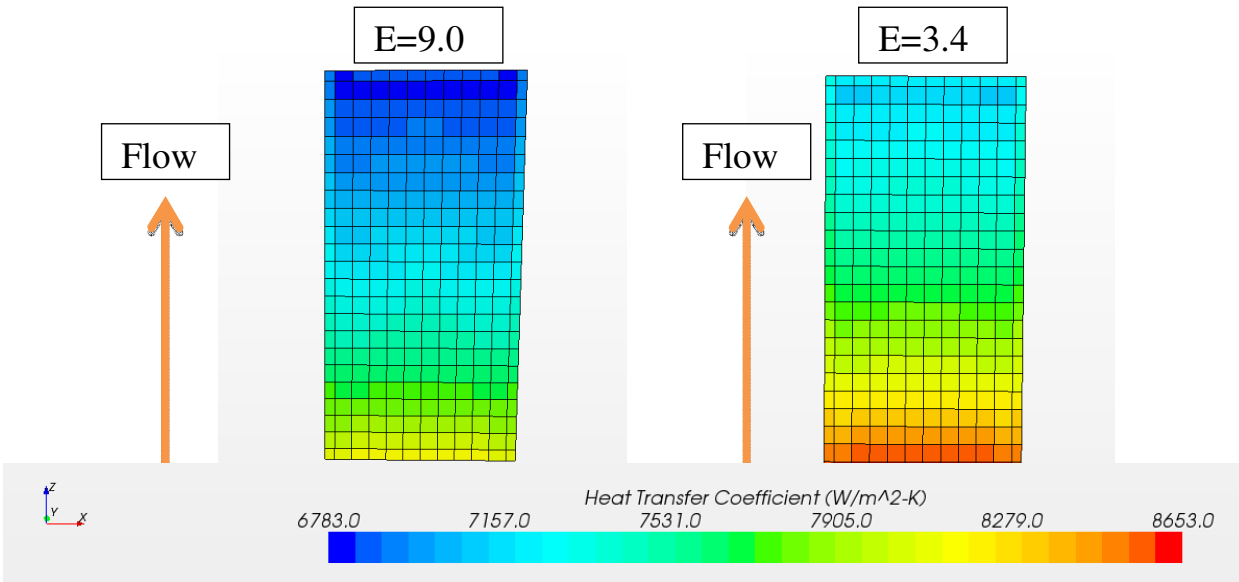

Figure 9 – Comparison of the heat transfer coefficient for a simulated smooth wall heater (left) versus a rough wall (right) to capture the effect of the presence of bubbles on the surface.

5. CONCLUSIONS AND FUTURE WORK

A fundamentally new wall boiling heat partitioningmodel that aims at extending the applicability and the accuracy of the approach to all boiling regimes and flow conditions is described here.The model is being developed with the support of new high-resolution experimental data to accurately represent the physical boiling phenomena that take place. In this work, the fundamental model structure and the initial formulation have been introduced. The primary target of the model is to correctly predict the temperatures and heat flux partitioning at the wall. The next step will be the implementation of the model in the STAR-CCM+ software and its evaluation on fundamental flow cases.

6. ACKNOWLEDGEMENTS

This work is supported by the Consortium for Advanced Simulation of Light Water Reactors (CASL) and the Elias P. Gyftopoulos Graduate Fellowship from MIT. In addition, special thanks is given to Bren Phillips, Rosie Sugrue, and Eric Forrest who have shared their experimental data and insight for the development of the model.

7. REFERENCES

[1] C. Gerardi, J. Buongiorno, L.-W. Hu and T. McKrell, "Infrared Thermometry Study of Nanofluid Pool Boiling Phenomena," *Nanoscale Research Letters,* vol. 6, no. 232, 2011.

[2] J. Garnier, E. Manon and G. Cubizolles, "Local Measurements on Flow Boiling of Refrigerant 12 in a Vertical Tube," *Multiphase Science and Technology,* vol. 13, pp. 1-111, 2001.

[3] T. Theofanous and T. Dinh, "High Heat Flux Boiling and Burnout as Microphysical Phenomena: Mounting Evidence and Opportunities," *Multiphase Science and Technology,* vol. 18, no. 3, pp. 251-276, 2006.

[4] V. Tolubinsky and D. Kostanchuk, "Vapour bubbles growth rate and heat transfer intensity at subcooled water boiling," in *Heat Transfer 1970, Preprints of papers presented at the 4th International Heat Transfer Conference*, Paris, 1970.

[5] G. Kocamustafaogullari, "Pressure dependence of bubble departure diameter for water," *Int. Comm. Heat Mass Transfer,* vol. 10, pp. 504-509, 1983.

[6] R. Cole, "A photographic study of pool boiling in the region of the critical heat flux," *AIChE J.,* vol. 6, pp. 533-542, 1960.

[7] N. Basu, G. R. Warrier and V. K. Dhir, "Wall Heat Flux Partitioning During Subcooled Flow Boiling: Part 1- Model Development," *Journal of Heat Transfer,* vol. 127, no. 2, pp. 131-140, 2005.

[8] N. I. Kolev, "How Accurately can We Predict Nucleate Boiling?," *Experimental Thermal and Fluid Science,* vol. 10, no. 3, pp. 370-378, 1995.

[9] T. Hibiki and M. Ishii, "Active nucleation site number density in boiling systems," *Int. J. Heat Mass Transfer,* vol. 46, pp. 2587-2601, 2003.

[10] G. Yeoh, S. Cheung, J. Tu and M. Ho, "Modeling Vertical Subcooled Boiling Flows at Low Pressures," *Journal of ASTM International,* vol. 8, pp. 1-20, 2011.

[11] R. Judd and K. Hwang, "A comprehensive model for nucleate boiling heat transfer including microlayer evaporation," *J Heat Transfer,* vol. 115, pp. 955-962, 1976.

[12] N. Kurul and M. Podowski, "Multidimensional effects in sub-cooled boiling," in *Proceedings of the Ninth Heat Transfer Conference*, Jerusalem, 1990.

[13] G. H. Yeoh and J. Tu, Computational Techniques for Multi-Phase Flows, Elsevier, 2010.

[14] M.-O. Kim, J. Tu, G. H. Yeoh and G.-C. Park, "On Population Balance Approach for Subcooled Boiling Flow Prediction," *Journal of Heat Transfer,* vol. 127, pp. 253-264, 2005.

[15] T. Lee, G. Park and D. Lee, "Local Flow characteristics of Subcooled Boiling Flow of Water in a Vertical Concentric Annulus," *International Journal of Multiphase Flow,* vol. 28, no. 8, pp. 1351-2368, 2002.

[16] J. F. Klausner, R. Mei, D. Bernhard and L. Zeng, "Vapor Bubble Departure in Forced Convection Boiling," *International Journal of Heat and Mass Transfer,* vol. 36, no. 3, pp. 651-662, 1993.

[17] L. Zeng, J. Klausner, D. Bernhard and R. Mei, "A Unified Model for the Prediction of Bubble Detachment Diameters in Boiling Systems- II. Flow Boiling," *International Journal of Heat and Mass Transfer,* vol. 36, no. 9, pp. 2271-2279, 1993.

[18] B. Yun, A. Splawski, S. Lo and C.-H. Song, "Advanced Wall Boiling Model for the Subcooled Boiling Flow with CFD Code," in *The Seventh Korea-Japan Symposium on Nuclear Thermal Hydraulics and Safety*, Chuncheon, Korea, 2010.

[19] W. E. Ranz and W. Marshall, "Evaporation from drops--Part I and II," *Chemical Engineering Progress,* vol. 48, p. 141, 1952.

[20] M. Salcudean and E. Bibeau, "A Study of Bubble Ebullition in Forced-Convection Subcooled Nucleate Boiling at Low Pressure," *International Journal of Heat and Mass Transfer,* vol. 37, no. 15, pp. 2245-2259, 1994.

[21] R. Situ, T. Hibiki, M. Ishii and M. Mori, "Bubble Lift-Off Size in Forced Convective Subcooled Boiling Flow," *International Journal of Heat and Mass Trasnfer,* vol. 48, pp. 5536-5548, 2005.

[22] J. Kim, "Review of Nucleate Pool Boiling Heat Transfer Mechanisms," *International Journal of Multiphase Flow,* vol. 35, no. 12, pp. 1067-1076, 2009.

[23] H. Kim and J. Buongiorno, "A Novel Infrared-Based Experimental Technique to Detect Phase Dynamics on Boiling Surfaces," in *Proceedings of the 11th International Topical Meeting on Nuclear Reactor Thermal-Hydraulics (NURETH-14)*, 2011.

[24] C. Gerardi, J. Buongiorno, L. Hu and T. McKrell, "Study of Bubble Growth in Water Pool Boiling Through Synchronized, Infrared Thermometry and High-Speed Video," *International Journal of Heat and Mass Transfer,* vol. 98, no. 4, pp. 4185-4192, 2010.

[25] V. H. DelValle and D. Kenning, "Subcooled Flow Boiling in High Heat Flux," *International Journal of Heat and Mass Transfer,* vol. 28, no. 10, pp. 1907-1920, 1985.

[26] D. Chatzikyriakou, D. Caviezel, J. Buongiorno and D. Lakehal, "ITM Test Case 1: LES and DNS of turbulent flow in a closed channel with flat walls featuring a pattern of small hemispherical solid obstacles," Cambridge, MA, 2011.